# Characterisation of chromium nitride films produced by PVD techniques

A. Barata, L. Cunha, C. Moura*

*Departamento de Física, Universidade do Minho, Campus de Gualtar, 4710-057 Braga, Portugal*

### Abstract

Chromium nitride thin films have been deposited on stainless steel substrates by r.f. reactive magnetron sputtering. The influence of process parameters such as substrate bias and partial pressure of reactive gas have been investigated. The characterisation of the coatings was performed by X-ray diffraction (XRD), Raman Spectroscopy (RS) and nano-indentation experiments. These studies allow to analyse the influence of deposition parameters in crystal phases, crystal orientation/texture and crystallite size. The relationship between structural defects and their characteristics with deposition conditions will also be taken into account. The presence of oxygen on the coatings surface, due to atmospheric contamination, is analysed by means of Raman spectroscopy. This optical technique can be used for the characterisation of the surface oxides at different stages of oxidation. The changes observed in Raman spectra can be correlated with process parameters. Coatings produced with an unbiased substrate showed higher tendency to surface oxidation. Increasing the nitrogen partial pressure in the working atmosphere produces changes from a hexagonal $Cr_2N$ to cubic CrN microstructure. The strain in CrN crystals increases with nitrogen content in working atmosphere. When the $Cr_2N$ phase is dominant the hardness has a relative maximum (42.2 GPa), but the highest hardness was obtained for a coating with dominant CrN phase produced with highest nitrogen flow (44.9 GPa). © 2001 Elsevier Science B.V. All rights reserved.

*Keywords:* Chromium nitride; Physical vapour deposition (PVD); Raman scattering

## 1. Introduction

Nitride coatings deposited by PVD techniques are well established to mechanically and chemically protect materials surfaces. Chromium nitride coatings have been studied in more detail during recent years. The protective capability of these nitrides strongly depends on the deposition conditions [1]. The hardness of chromium nitride coatings depends also on the nitrogen content related with the formation of $Cr_2N$ phase [2]. Friction properties are a consequence of structure and orientation of crystals in the film [3]. The corrosion properties are dependent of the porosity/density of the coatings [4,8]. The importance of the deposition parameters is critical.

Chromium nitride coatings were deposited by r.f. magnetron sputtering varying working gas composition and substrate bias. X-Ray diffraction was used to study the microstructure/texture and grain size.

Raman spectroscopy is a non-destructive technique that gives information about vibrational modes of materials and can be used in a complementary manner with other traditional techniques used in thin films characterisation. The Raman effect is related with vibration-induced changes in the electronic polarisability of a molecular system. Many transition-metal borides, carbides and nitrides crystallise in the cubic system with sodium–chloride-type structures. In these ideal crystals the first order Raman scattering is forbidden. Nevertheless hard coatings are known to have vacancies due to deficiency of one component and these defects induced distortion on the structure and first order Raman scattering could be observed. The spectra are composed by peaks or bands belonging to first order scattering and second order scattering due to combinations of first order modes [5,6].

* Corresponding author. Tel.: +351-253-604332; fax: +351-253678981.

*E-mail address:* cacilda@fisica.uminho.pt (C. Moura).

Table 1
Some deposition parameters: substrate bias ($V_S$); nitrogen flow [$\Phi(N_2)$], coating thickness ($t_C$); composition; crystallite size [* — measured in Cr (200) peak, † — measured in CrN (111) peak]; interplanar distance ($d$); strain ($\varepsilon$); lattice parameter ($a$); nano-hardness; and Young's modulus. The crystallite size and lattice parameters couldn't be measured with enough accuracy to be registered in this work (−)

| Sample | $V_S$ [V] | $\Phi(N_2)$ [sccm] | $t_C$ [μm] | Composition [%]±3% Cr | N | Crystallite size [nm] | Cr(200) $d$ [Å] | $\varepsilon$[%] | $a$ [Å] | CrN(111) $d$ [Å] | $\varepsilon$[%] | $a$ [Å] | Hardness [GPa] | Young's Modulus [GPa] |
|---|---|---|---|---|---|---|---|---|---|---|---|---|---|---|
| JCPDS | − | − | − | − | − | − | 1.4419 | − | 2.8839 | 2.394 | − | 4.1465 | − | − |
| A7/1 | −50 | 0 | 8.6 | 100 | 0 | ~30* | 1.4464 | 0.31 | 2.8927 | − | − | − | 10.0 | 447 |
| B7/2 | −50 | 2 | 5.5 | 90 | 10 | ~7* | 1.4520 | 0.70 | 2.9039 | − | − | − | 42.2 | 547 |
| B3/1 | −50 | 2.4 | 4.0 | 88 | 12 | ~4* | 1.4564 | 1.01 | 2.9129 | − | − | − | 39.2 | 475 |
| A8/2 | −50 | 10 | 5.5 | 60 | 40 | − | − | − | − | − | − | − | 16.8 | 376 |
| A9/1 | −50 | 20 | 4.2 | 50 | 50 | ~12† | − | − | − | 2.4288 | 1.45 | 4.2068 | 27.1 | 380 |
| A10/1 | −50 | 30 | 3.1 | 50 | 50 | ~13† | − | − | − | 2.4362 | 1.76 | 4.2197 | 26.9 | 358 |
| A6/1 | −50 | 40 | 2.8 | 50 | 50 | ~16† | − | − | − | 2.4532 | 2.47 | 4.2490 | 37.6 | 437 |
| A14/1 | −50 | 50 | 2.9 | 50 | 50 | ~18† | − | − | − | 2.4531 | 2.47 | 4.2489 | 41.1 | 476 |
| A15/1 | −50 | 60 | 2.5 | 50 | 50 | ~18† | − | − | − | 2.4575 | 2.65 | 4.2566 | 44.9 | 486 |
| B8/1 | 0 | 2 | 5.9 | 90 | 10 | ~5* | 1.4597 | 1.23 | 2.9194 | − | − | − | 34.9 | 454 |
| B4/1 | 0 | 2.4 | 4.6 | 88 | 12 | − | − | − | − | − | − | − | 36.2 | 459 |
| A11/1 | 0 | 40 | 4.3 | 50 | 50 | ~10† | − | − | − | 2.4028 | 0.37 | 4.1618 | 5.8 | 163 |

## 2. Experimental

### 2.1. Coatings deposition

The coatings were deposited by reactive r.f. magnetron sputtering on stainless steel substrates. The substrates were previously ultra-sonically cleaned in acetone and sputter etched in a pure argon atmosphere. The target to substrate distance was kept constant at 65 mm. The coatings were produced from pure chromium target and argon/nitrogen atmosphere. The argon flow was constant (60 sccm). The samples were produced with different nitrogen flow (from 0 to 60 sccm). The target power was 500 W. Most of the coatings were deposited with a substrate bias of −50 V but some were produced with grounded substrate. The substrate temperature during deposition was 300°C. The thickness of the coatings was obtained by ball cratering and the composition was obtained by Rutherford backscattering spectroscopy (RBS). The deposition conditions and some of the coatings properties are summarised in Table 1.

### 2.2. Coating characterisation

#### 2.2.1. X-Ray diffractometry

The diffraction patterns were recorded in a classical $\theta/2\theta$ difractometer, with a Bragg–Brentano geometry using CuK$\alpha$ radiation. The step size was 0.02° $2\theta$, with 1.25 s/step. Fitting XRD peaks by a pseudo–Voigt function revealed the grain size [7]. This method needs only a diffraction peak and is based on the fact that the experimental profile is the convolution of structural and experimental profiles. The crystallite size calculations were performed by making corrections due to the CuK$\alpha_2$ component and instrumental profile.

#### 2.2.2. Raman scattering

Raman spectra measurements were made using a T64000 Jobin–Yvon triple monochromator with a CCD detector. An argon ion laser operating with 488-nm and 514.5-nm lines, with power levels onto the sample of 20 and 40 mW, respectively, was used as a light source. The measurements were performed with a BHSM Olympus microscope using ×50 and ×100 MS Plan objectives. The spectra were collected during 200 s from 100–2000 cm$^{-1}$ with a spectral resolution of approximately 2.5 cm$^{-1}$.

#### 2.2.3. Hardness measurements

The nano-hardness was determined using a Berkovich indenter with instrumented indentation depths of 100, 200 and 300 nm. The hardness is considered to be the average of the measurements with indentation depths of 100 nm, in order to minimise the substrate influence. These measurements also permitted to determine the Young's modulus.

## 3. Results and discussion

### 3.1. Phase identification and crystallite size

The XRD patterns of the coatings show differences according deposition conditions. When there is no nitrogen flow (sample A7/1), only chromium peaks are detected. There is a strong (200) reflection, but (110) and (211) are also clearly defined. The peaks are shifted to lower $2\theta$ values. This evidence is found in all studied samples. The positive deviation of interplanar spacings and lattice parameter, when compared with JCPDS reference values, indicates a compressive residual stress [8] (see Table 1). The crystallite size calculated from
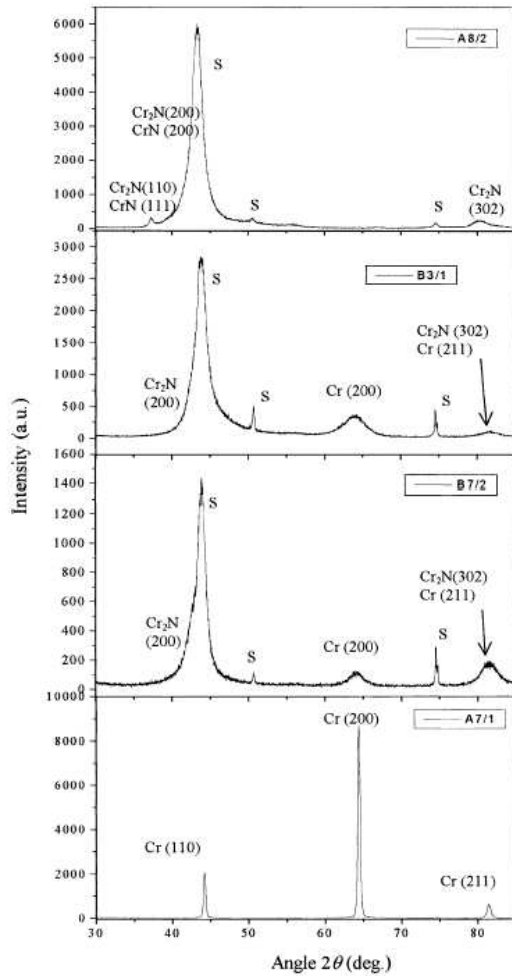
Fig. 1. The XRD patterns of samples deposited with low $\Phi$ (N$_2$) [0 < $\Phi$(N$_2$) < 10 sccm] and biased substrate (S — substrate peaks).

broad peaks), but may be attributed to the CrN, Cr$_2$N and probably Cr$_x$N$_y$ phases.

With flows of nitrogen above 10 sccm, only the CrN phase is present. The detected peaks correspond to reflections on planes (111), (200), (220), (311) and (222), depending on the deposition conditions. The most intense peaks correspond always to reflections on CrN (111) planes (Fig. 2).

Above a flow of 40 sccm, the shifts to lower angular positions are very strong which means that high stresses
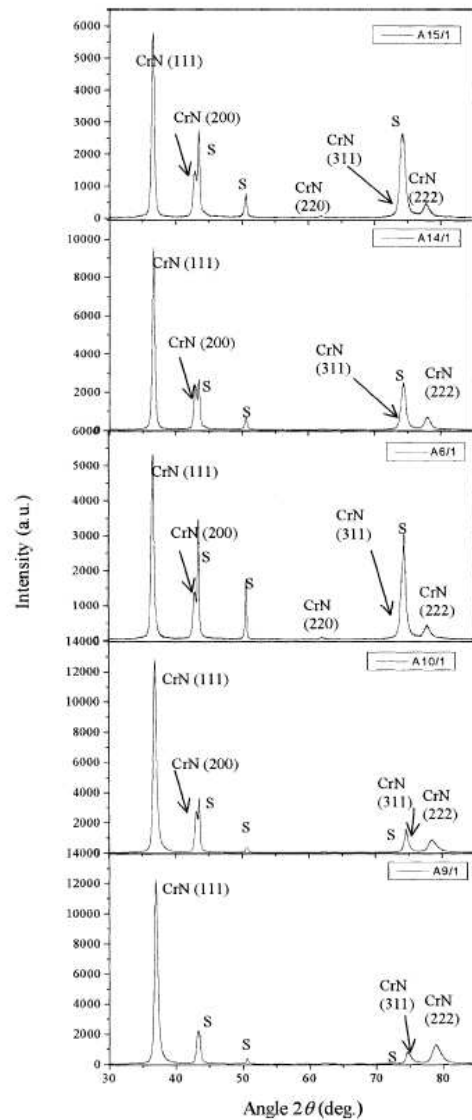
the peak corresponding to (200) planes is approximately 30 nm.

Increasing the nitrogen flow to 2 sccm (sample B7/2) and 2.4 sccm (sample (B3/1), produces coatings with weak diffraction peaks and peak broadening (see Fig. 1), probably due to small crystallite size (between 4 and 6 nm) and insertion of nitrogen atoms which may cause higher non-uniform stresses. The Cr (200) peak detected in each one of these samples shows higher shifts to lower 2θ values. We may also have Cr$_2$N phase, confirmed by Raman scattering. There is superposition of diffraction peaks corresponding to Cr$_2$N (200), CrN (200) planes and substrate peak at 2θ at approximately 43°. With 10 sccm the diffraction pattern still shows disorganisation of the structure (weak and



Fig. 2. The XRD patterns of samples deposited with high $\Phi$ (N$_2$) [20 sccm < $\Phi$(N$_2$) < 60 sccm) and biased substrate (S — substrate peaks).
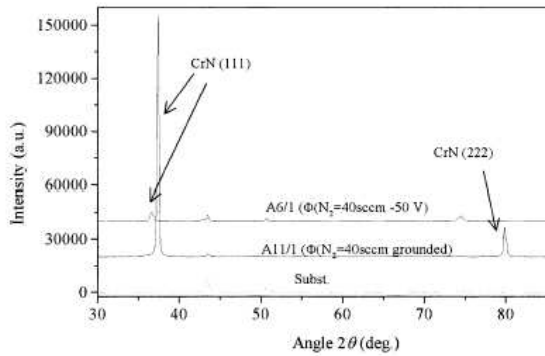
Fig. 3. The XRD patterns of samples deposited with nitrogen flow $\Phi(N_2) = 40$ sccm and a substrate bias of $-50$ or $0$ V.

are present. This strong shift may be caused by insertion of nitrogen atoms in the CrN structure. For these samples the grain size is calculated to be between 15 and 20 nm, using the peak corresponding to (111) planes.

Comparing X-ray diffraction patterns of coatings deposited with $-50$ V substrate bias with those obtained with the samples deposited with grounded substrate, no significant differences are observed when the $\Phi(N_2)$ is low (2 or 2.4 sccm). If the nitrogen flow is significant (40 sccm), the samples show texture with (111) planes parallel to surface and the shift is lower, as expected for a grounded substrate deposition [8] (see Fig. 3). These results are the consequence of less intense ion bombardment during deposition. The calculated grain size for the grounded deposited samples is approximately 5 and 10 nm.

According to the XRD data, with increasing percentage of reacting gas in the working atmosphere, the dominant Cr phase changes to coatings with mixed Cr, $Cr_2N$ and probably $Cr_xN_y$ phases when the quantity of nitrogen is low. For higher nitrogen contents in the working atmosphere the CrN phase is dominant. The lattice parameter measured in the direction perpendicular to the coating surface is significantly larger for the coatings deposited with the nitrogen richest atmospheres and substrate bias of $-50$ V (A6/1, A14/1 and A15/1). This also means that these coatings are highly stressed (compressive residual stress). The dominant phases for the samples deposited without bias are similar to the correspondent coatings produced with substrate bias but in general with lower residual stresses.

### 3.2. Raman scattering

The phonon frequency observed in Raman scattering is proportional to $(k/m)^{1/2}$, where $k$ is an effective force constant between atoms and $m$ is the correspondent reduced mass. Chromium and titanium nitride have the same parameter of cell and the Young's modulus is of

the same magnitude. It is expected that the effective force constant between Cr–N bonds and Ti–N bonds be of the same magnitude. In consequence we may expect that CrN presents, in RS, the same behaviour that has been observed in other nitride coatings like TiN or ZrN. In fact all of these coatings crystallise with the same structure, f.c.c. TiN has approximately the same density and molecular weight of CrN and in consequence the Raman spectra will present the same trends.

Moreover, it is known that chromium nitride can crystallise as $Cr_2N$ in a hexagonal phase [9]. This compound belongs to the $D_{3d}^1$ group symmetry [10], with three molecules per unit cell, presenting 5 active modes in Raman scattering: $2A_{1g} + 3E_g$.

Raman scattering was made with the samples where $\Phi(N_2)$ changes from 2 to 60 sccm. In Fig. 4 the Raman spectrum of sample B7/2, which has been prepared with lower nitrogen content, is reported. Its known that when the $\Phi(N_2)$ is lower, $Cr_2N$ is the major compound deposited [9]. Even if there is no report, to our knowledge, of RS in chromium nitride, we think that the observed features in the Raman spectra can be assigned to $Cr_2N$ phase where we denote five active modes at 215, 267, 284, 385 and 490 cm$^{-1}$ and bands due to second order combinations at 586, 667, 760 and 943 cm$^{-1}$.

With an increasing fraction of nitrogen in the sputtering gas the Raman spectra of nitride coatings show a change from the hexagonal to cubic chromium nitride phase. In fact some of the features seen in sample B7/2 disappear or are shifted to lower frequencies as the nitrogen content increases. In addition we have seen in RS of samples A8/1 that it contains modes due to h-CrN and c-CrN indicative that both phases could be present, like it is assigned by the XRD results. In Fig. 5 we report the spectrum of sample A14/1, that present an intense peak at 223 cm$^{-1}$ bands at 330, 460, 660, 910 and 1050 cm$^{-1}$. The very intense peak could been
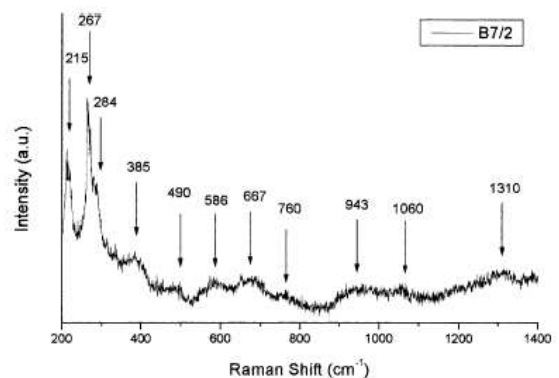


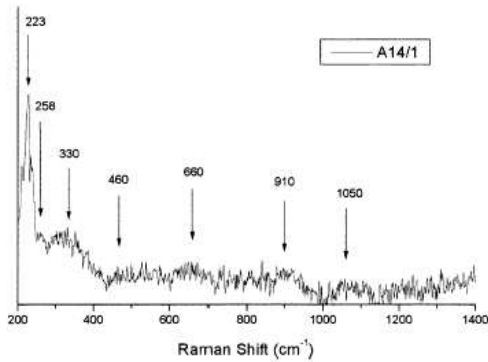Fig. 4. Raman spectrum of coating with dominant h-$Cr_2N$ phase (B7/2).

Fig. 5. Raman spectrum of coating with dominant c-CrN phase (A14/1).

assigned to a resonance Raman effect, of asymmetric stretching vibration of $Cr_3$, since it has been observed in matrices containing Cr prepared by evaporation [11]. The other large bands are contributions from c-CrN phase in similarity with the observations made on other nitride coatings.

Like in TiN, we assume that the vibrations in the acoustic frequency range (typically 200–300 $cm^{-1}$) are mainly due to the vibrations of metal atoms, while the vibrations of lighter non-metal ions dominates the optical range (typically 400–650 $cm^{-1}$). If the samples are non-stoichiometric, the missing of nitrogen atoms reduces the number of vibrations and in consequence the scattering in the optical range is small, as we can see in spectrum represented in Fig. 4.

Raman spectra from films deposited at 0 V bias showed peaks at 305, 342, 540, 597 $cm^{-1}$, characteristic of $Cr_2O_3$ [12], indicating that some oxidation on the films surface takes place [13] due to atmospheric contamination. This higher oxidation of grounded deposited films is probably due to higher porosity of these coatings when compared to those deposited with negatively biased substrate [8].

### 3.3. Hardness and Young's modulus

In general, comparing the samples produced with biased substrate, when the nitrogen flow increases, the hardness of the coatings also increases (see Fig. 6), but there are significant variations. With no nitrogen flow (A7/1), the chromium coating hardness is approximately 10 GPa. With a flow of nitrogen of 2 (B7/2) and 2.4 sccm (B3/1), the hardness strongly increases to 42 and 39 GPa, respectively. With a 10-sccm nitrogen flow (A8/2) the hardness decreases to approximately 17 GPa. Then the hardness increases almost linearly with the increase of nitrogen flow. The maximum hardness

(45 GPa) was obtained for the coating produced with 60 sccm nitrogen flow (A15/1).

The reason for the exceptional hardness of coatings of sample B7 and B3 may be found in the small grain size and also of the presence of $Cr_2N$ phase, detected by XRD and RS, whose hardness is higher [2] when compared with coatings with dominant CrN phase.

The increase of the hardness in the coatings with dominant CrN phase, when the nitrogen flow increases from 20 to 60 sccm may be related to an increase of compressive residual stress.

The coatings produced with grounded substrate have lower hardness than the coatings produced with negative bias. This result is expected because these coatings are usually less dense and their porosity is higher [4,8]. Nevertheless, this difference is almost negligible for the coatings produced with low nitrogen flow (B8/1–2 sccm and B4/1–2.4 sccm), but it is significant when the nitrogen flow is high (A11/1–40 sccm). The reason for this behaviour may be due to the presence of the $Cr_2N$ phase and lower grain size when compared with sample A11/1.

The Young's modulus of the samples is a result of the nano-indentation experiments and the variation of this property (measured perpendicularly to sample surface) with deposition parameters is similar to the variation of the nano-hardness.

### 4. Conclusions

The results of this work can be summarised as follows:

1. XRD data show that the structure of the phases changes from Cr to $Cr_2N$ and CrN with increasing nitrogen content in a working atmosphere. The diffraction peaks are always shifted to lower angles which means the presence of compressive residual
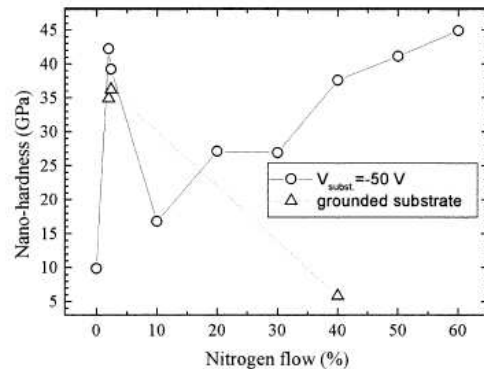


Fig. 6. Variation of the nano-hardness of the coatings with nitrogen flow.

stresses. When ion energy is lower (during grounded depositions) the f.c.c. crystals of CrN tend to be (111) oriented and the stress and strains are lower. With increasing ion bombardment, other orientations appear, but the dominant is (111) planes parallel to sample surface.

2. The Raman spectra of the analysed chromium nitride films suggest a change from hexagonal to cubic phase of chromium nitride when the content of nitrogen increases. The observed Raman scattering in the cubic phase is induced by the existence of defects in the structure, like N vacancies, which enable the observation of Raman diffusion. Much more work must be done, theoretical and experimental, to complete these observations. Moreover, the samples deposited with grounded substrate are more susceptible to oxidation when in contact with the atmosphere.

3. The hardness and Young's modulus of the coatings with dominant CrN phase increases with the increase of nitrogen flow during deposition. One of the reasons may be the increase of compressive residual stress due to the insertion of nitrogen atoms in the CrN structure. The maximum hardness was 44.9 GPa for the coating produced with the highest nitrogen flow. High hardness was also measured for the samples were $Cr_2N$ phases were detected. These samples exhibited a small crystallite size (4–6 nm).

## References

[1] R. Sanjinés, P. Hones, F. Lévy, Thin Solid Films 332 (1998) 225–229.
[2] M. Pakala, R.Y. Lin, Surf. Coat. Technol. 81 (1996) 233–239.
[3] J.P. Terrat, A. Gaucher, H. Hadj-Rabah, Surf. Coat. Technol. 45 (1991) 59–65.
[4] L. Cunha, M. Andritschky, L. Rebouta, K. Pischow, Surf. Coat. Technol. 116-119 (1999) 1152–1160.
[5] C.P. Constable, J. Yarwood, W.D. Munz, Surf. Coat. Technol. 116-119 (1999) 155–159.
[6] W. Spengler, R. Kaiser, A.N. Christensen, G. Muller-Vogt, Phys. Rev. B 17 (1978) 1095–1101.
[7] Th.H. de Keijser, J.I. Langford, E.F. Mittemeijer, A.B.P. Vogels, J. Appl. Crystallogr. 15 (1982) 308.
[8] L. Cunha, M. Andritschky, K. Pischow, Z. Wang, Thin Solid Films 355-356 (1999) 465–471.
[9] C. Meunier, S. Vives, G. Bertrand, Surf. Coat. Technol. 107 (1998) 149–158.
[10] D.L. Rousseau, R.P. Bauman, S.P.S. Porto, J. Raman Spectrosc. 10 (1981) 253–290.
[11] D.P. DiLella, W. Limm, R.H. Lipson, M. Moskovits, K.V. Taylor, J. Chem. Phys. 77 (1982) 5263–5266.
[12] T.R. Hart, R.L. Aggarwal, B. Lax, Proceedings of the 2nd International Conference in Light Scattering in Solids, Flammarion Science, Paris, France, 1971, pp. 174–179.
[13] S. Logthetidis, E.I. Meletis, G. Kouroukis, J. Mater. Res. 14 (1999) 436–441.